

Atmospheric Temperature Measurements by Aerodynamic and
Sound Propagation Techniques

John W. Peterson
High Altitude Engineering Laboratory
Department of Aeronautical and Astronautical Engineering
The University of Michigan
Ann Arbor, Michigan

For Presentation at
Fourth Symposium
on
Temperature, Its Measurement and Control in Science and Industry
Columbus, Ohio
27-31 March 1961

Abstract

Several methods exist for temperature measurement at altitudes greater than the balloon-sonde limit. A method for measuring air density or pressure over a range of altitudes is also a temperature method because these parameters are interrelated. Several recent measurements of this kind are discussed.

Drag effects on the orbit of an earth satellite are a measure of atmospheric density at perigee altitude. Density has been measured by satellites in the altitude range 200 to 700 kilometers. Large variations of density and temperature due to diurnal and solar effects have been found

The temperature of electrons in the ionosphere has been measured by a Langmuir probe technique.

The pitot-static tube technique has been used to measure density and pressure. Wind velocity has also been found by measuring the pressure on the side of a spinning rocket.

The rocket-grenade system measures the average speed of sound in the atmosphere between exploding grenades. Wind velocity can also be measured by this technique. Large seasonal temperature variations have been found at northern latitudes at high altitudes.

The aerodynamic drag on a falling sphere is a measure of atmospheric density. Accelerations due to drag have been found by differentiating trajectory data and by means of an accelerometer equipped sphere. Density profiles are shown for four wintertime flights at northern latitudes. Temperature plots derived from the density profiles show an abrupt warming in the atmosphere.

Introduction

The basic equations applicable to atmospheric structure are discussed. Three techniques for determining temperature at high altitude are described briefly. The rocket grenade system and the falling sphere system are described in more detail and the results of several rocket flights are shown.

I. Basic Equations

The direct determination of upper atmosphere temperature is generally unfeasible due to the lack of a satisfactory technique. However, a number of techniques exist for measuring density or pressure or both density and pressure. In the latter case the ideal gas equation of state may be used to derive the temperature.

$$T = \frac{MP}{R\rho} \quad (1)$$

The gas constant R is known and also the molecular mass M at low altitudes. The variation of M with altitude is insignificant up to the 120 kilometer level for most purposes. At higher altitudes the molecular mass is not precisely known but equation (1) can be used to determine the molecular-scale temperature defined by

$$T_M = \frac{M_0}{M} T = \frac{M_0}{R} \frac{P}{\rho} \quad (2)$$

The derivation of the true temperature T then depends upon the best estimate of M_0/M at hand.

The temperature can be derived from pressure data alone if an altitude profile is available. In this case one uses the barometric equation which states the equilibrium of gravitational forces.

$$dP = - \rho g dh \quad (3)$$

Equation (1) and (3) imply the desired temperature equation

$$\frac{d \ln P}{dh} = - \frac{Mg}{RT} \quad (4)$$

Equation (4) is useful for temperature determinations provided the quality of the pressure data is such that differentiation is practical.

The scale height H is defined by

$$H = \frac{RT}{Mg} \quad (5)$$

If the temperature and molecular weight are constant in a layer an exponential atmosphere results for which

$$\frac{P}{P_0} = \frac{\rho}{\rho_0} = e^{-\frac{h}{H}} \quad (6)$$

Temperature can also be derived from the density profile. According to equation (3) pressure can be derived by integrating the density so that

$$P = P_1 - \int_{h_1}^h \rho g dh \quad (7)$$

With both pressure and density at hand the temperature is found from equation (1). The initial pressure P_1 is known from balloon-sonde observations if integration begins at a low altitude. This procedure is impractical if the range of altitude is several scale heights because the final pressure will then be small compared to P_1 and errors become larger than the pressure calculated. Better results are obtained in practice if integration begins at the greatest altitude where the initial pressure must be assumed. In this case, integrating downward, the exponential increase of pressure tends to suppress an initial error. The initial pressure can be found by assuming initial temperature which is preferable because temperature can probably be estimated more accurately than pressure at high altitudes.

A somewhat more direct technique of temperature measurement depends upon the sound propagation equation

$$MC^2 = \gamma RT \quad (8)$$

where C is the speed of sound in air and γ is the ratio of specific heats.

II. Atmospheric Temperature Measurements

Newell¹ presented an excellent survey of this field at the Third Symposium on Temperature (1954). Subsequently these techniques have been exploited by many experimenters to provide new knowledge of the atmosphere. The International Geophysical Year stimulated much of this work.

A. Satellite Techniques

A new development since Newell's review has been the use of earth satellites. Properties of the upper atmosphere have been derived from the drag effect on the orbit of a satellite by Jacchia², King-Hele³, and others. Atmospheric density has been derived between the altitudes of 200 km and 700 km from the orbits of 1958β2 (Vanguard I), 1959α1 (Vanguard II), 1958α (Explorer I), and 1958 δ 2 (Sputnik III) by Jacchia.⁴ The measured quantity is the satellite secular acceleration dP/dt (non-dimensional) where P is the period of the orbit. Averages over 25 revolutions were taken in most cases. At low altitudes the method fails because the satellite spirals in at a rapid rate. At high altitudes the accelerations become vanishingly small.

King-Hele⁵ has derived an approximate formula relating satellite accelerations to orbital elements and atmospheric parameters, namely:

$$\rho \sqrt{H} = \frac{1}{3 C_D} \sqrt{\frac{2}{\pi}} \frac{m}{AF} \left(-\frac{dP}{dt} \right) \frac{e}{a} \left[1 - 2e + 2.5e^2 - \frac{H}{8ae} (1 - 10e + \frac{7H}{16ae}) \right] \quad (9)$$

where

- ρ = atmospheric density at satellite perigee height.
- H = atmospheric scale height near perigee
- C_D = drag coefficient (2.0)
- m = mass of satellite
- A = effective cross-section of satellite
- F = factor to account for rotation of atmosphere
- e = orbital eccentricity
- a = semi-major axis of satellite orbit

Drag effects are localized near perigee because atmospheric density decreases rapidly with altitude. Satellite accelerations are also a measure

of the scale height because an increased scale height enlarges the portion of the orbit which is in dense air. If the product ρ/H is known as a function of altitude a determination of ρ and H separately is possible.

An elliptical orbit is useful for detecting diurnal effects. A perfectly circular orbit is not as satisfactory because it measures an average density on the sunlit and shadowed portions of the earth. The perigee of an eccentric orbit will appear over different points of the earth each revolution but it tends to remain in the same position relative to the earth-sun axis. The annual motion of the earth about the sun and also drag effects will cause the perigee to move slowly between sunlit and shadowed areas, Figure 1. Diurnal changes can be observed if the lifetime of the satellite is many hundreds of revolutions.

The first earth satellites revealed that atmospheric density at satellite altitudes was larger than had been commonly accepted by an order of magnitude. This implies a warmer atmosphere since temperature governs the rate at which density decreases with altitude.

Jacchia⁴ has found a bulge in the atmosphere on the sunlit side of the earth due to heating effects of the sun. The diurnal variation of density is a factor of ten at the 700 kilometer level but is small at 200 kilometers. The bulge appears to be centered at the latitude of the subsolar point but lags in longitude by 25 to 30 degrees. Fluctuations of comparable magnitude have been measured which are correlated with the 27 day period of solar rotation. Increases in density during magnetic storms have also been inferred from satellite accelerations.

B. Electron Temperature

Bogges, Brace, and Spencer⁶ have measured electron temperature through the use of a rocket-borne adaptation of a Langmuir probe. Two 6-in spheres were used separated by a 10-in long $2\frac{1}{4}$ in diameter cylinder. Each sphere was composed of two electrically insulated hemispheres; the outer hemispheres acted as information electrodes, and the inner ones as guard electrodes. The electron temperature is obtained from the slope of a plot of logarithm of current vs. voltage. Maxwell-Boltzmann energy distribution must be assumed. The volt-ampere curve is obtained by measuring the current between information electrodes as the voltage is varied. Electron temperatures were measured from 111 to 177 kilo-

meters. More recent work⁷ has extended the measurements to an altitude of 440 kilometers. The electron temperature profile appears to have the same general characteristics as the gas temperature profile.

C. Pitot-Static Tube Measurements

Ainsworth, Fox, and LaGow⁸ have measured atmospheric pressure and density using the pitot-static tube. A wide range of pressures are measured by using 3 mechanical diaphragm type gauges of different sensitivities. The Rayleigh pitot formula was used to determine ambient density

$$\rho = \frac{1}{V^2} (0.144 P_i - 0.066 P) \quad (10)$$

$$\left[\frac{\text{gm}}{\text{m}^3} = \frac{\text{mm Hg}}{\left(\frac{\text{km}}{\text{sec}}\right)^2} \right]$$

where P_i is the impact pressure measured at the nose of the tube, P is the ambient pressure in a space fed by several orifices in the side of the tube, and V is the velocity of rocket.

At higher altitudes a free-molecular-flow equation was used:

$$\rho = \frac{P_i}{\sqrt{\pi} u' |V| \cos \psi} \quad (11)$$

where u' is the most probable velocity of the molecules in the tube and ψ is the effective angle of attack of the rocket. Temperature was computed in three ways, from the equation of state, from the pressure profile, and from the density profile. This technique has been successful to altitudes as high as 110 kilometers.

Spin pressure was measured by a single orifice in the side of the rocket. This pressure is modulated by the spin rate of the rocket, in this case 1.7 cps. It is possible to derive the horizontal component of wind velocity from the spin pressure data. Aspect of the rocket must also be measured in order to determine winds.

D. The Rocket-Grenade System

Equation (8) is the basis of rocket-grenade measurements of upper air temperature. The sound waves generated by exploding grenades at high altitudes are detected by microphones on the ground. If n grenades are used the average temperature in $n-1$ layers of the atmosphere can be found. The horizontal component of wind in these layers can also be determined if the inclination on arrival of each wave front is known. An array of several microphones on the ground is used to determine the inclination. It is difficult to separate the effects of vertical wind and temperature but this is not believed to be an important source of error. According to equations (4) and (1) pressure and density profiles can be constructed from the temperature profiles. The low air density at high altitude dissipates the energy of a sound wave as it propagates. This effect sets an altitude limit of approximately 95 kilometers for the grenade technique. An accurate determination of position in space of each explosion is needed. This has been accomplished by photographing grenade explosions against a star background using several ballistic cameras. The DOVAP tracking system can also be used to establish coordinates of explosions. In this case, the grenades are exploded a measured distance in front of the rocket using a lanyard. Use of DOVAP removes the limitation of clear skies necessary for ballistic cameras.

Rocket-grenade measurements have been carried out at White Sands⁹, Fort Churchill¹⁰, and Guam¹¹. The Fort Churchill and Guam work was part of the United States IGY program. The Aerobee rockets at Fort Churchill carried 19 grenades, Figures 2 and 3. Each grenade exploded at high altitude contained 4 pounds of high explosive. At low altitude 2-pound grenades were used. At Guam Nike-Cajun rockets carried five 1-pound grenades and five 2-pound grenades. The grenade explosions are spaced at approximately 3 kilometer levels of altitude.

Figures 4 and 5 show summer and winter temperature profiles at Fort Churchill, Canada (latitude 59°N) compared with White Sands, New Mexico (latitude 33°N). These profiles show a winter temperature higher and summer temperature lower than the White Sands average at high altitude. No seasonal temperature variations were found at White Sands.

Further grenade measurements using Nike-Cajun rockets are being made by the University of Michigan, and National Aeronautics and Space Administration as a combined effort.

E. The Falling Sphere System

The drag induced acceleration of a falling sphere is a measure of atmospheric density according to the equation

$$m a_D = C_D A \frac{1}{2} \rho V^2 \quad (12)$$

where m is the mass of the sphere and A its cross-sectional area. Temperature can be derived from the density profile according to equations (1) and (7). The drag acceleration has been derived from DOVAP trajectory data¹² and also has been measured by an accelerometer in the sphere¹³, Figure 6. The latter method has proved to be most satisfactory because of increased sensitivity and simplicity. It is possible to determine sphere velocity and the altitude at which data is taken by integrating measured accelerations so that radar or other tracking systems are not required.

Wind tunnel and ballistic range measurements indicate a variable drag coefficient depending on the Reynolds Number and Mach Number. At the highest altitudes the drag coefficient approaches 2.0, a value often assumed for satellites. As the sphere falls to lower levels the Reynolds Number increases and the drag coefficient falls to 0.90. At approximately 18 kilometers where the velocity approaches subsonic, a condition of unsteady drag is observed, and measurements become unreliable. The low altitude end of the sphere data usually overlaps the high altitude end of the balloon-sonde data. The peak altitude of the sphere trajectory is determined by matching the two density profiles.

Measurements of upper-air densities and temperatures from 12 sphere flights have been reported¹⁴. A latitude survey was carried out by a series of rocket firings from a ship. In this case no tracking radar was available. This survey was made possible by the relative simplicity of the sphere system which does not require radar. Figure 7 shows the density measured by four spheres at Fort Churchill, Canada in winter. Temperatures derived from the density profiles are shown in Figure 8. The high temperatures measured by AM 6.03 are due to the phenomenon of abrupt warming which is known to occur rather infrequently in winter at northern latitudes¹⁵. Rocket SM 2.10 carried grenades as well as the sphere permitting a comparison of temperatures measured by the two methods, Figure 9.

Further development of the sphere system continues at the University of Michigan supported by the Air Force, Geophysics Research Directorate. A more sensitive accelerometer has been designed in order to extend measurements to higher altitudes.

Acknowledgements

I should like to thank L. M. Jones and F. L. Bartman for their helpful discussions.

REFERENCES

1. Newell, H. E., Jr., "Temperature, Its Measurement and Control in Science and Industry", Edited by Hugh C. Wolfe, Reinhold Publishing Corp., 429-444 (1955).
2. Jacchia, L. G. "Two Atmospheric Effects in the Orbital Acceleration of Artificial Satellites", *Nature*, 183, 526-527 (1959).
3. King-Hele, D. G., and Walker, D. M. C., "Irregularities in the Density of the Upper Atmosphere: Results from Satellites" *Nature*, 183, 527-530, (1959).
4. Jacchia, L. G. "A Variable Atmospheric Density Model from Satellite Accelerations", *Journal of Geophysical Research*, 65, 2775-2782 (1960).
5. King-Hele, D. G., Cook, G. E., and Walker, D. M. C., "Contraction of Satellite Orbits Under the Influence of Air Drag, Part I" Royal Aircraft Establishment (Farnborough) Tech. Note G. N. 533.
6. Boggess, R. L., Brace, L. H., and Spencer, N. W., "Langmuir Probe Measurements in the Ionosphere", *Journal of Geophysical Research*, 64, 1627-1630, (1959).
7. Personal Communication, L. H. Brace, Department of Electrical Engineering, University of Michigan
8. Ainsworth, J. E., Fox, D. F. and LaGow, H. E., "Measurement of Upper-Atmosphere Structure by Means of the Pitot-Static Tube", NASA TN D-670, (1961).
9. Stroud, W. G., Nordberg, W., and Walsh, J. R., "Atmospheric Temperatures and Winds Between 30 and 80 Km", *Journal of Geophysical Research*, 61, 45-56 (1956).
10. Stroud, W. G., Nordberg, W., Bandeen, W. R., Bartman, F. L. and Titus, P., "Rocket-Grenade Measurements of Temperatures and Winds in the Mesosphere over Churchill, Canada", *Journal of Geophysical Research*, 65, 2307-2323, (1960).
11. Nordberg, W., and Stroud, W. G., "Results of IGY Rocket-Grenade Experiments to Measure Temperature and Winds Above the Island of Guam", *Journal of Geophysical Research*, 66, 455-464, (1961).

REFERENCES (continued)

12. Bartman F. L., Chaney, L. W., Jones, L. M. and Liu, V. C.
"Upper-Air Density and Temperature by the Falling Sphere Method", *Journal of Applied Physics*, 27, 706-712, (1956).
13. Jones, L. M., Peterson, J. W., Schaefer, E. J., and Schulte, H. F.
"Upper-Air Densities and Temperatures from Eight IGY Rocket Flights by the Falling-Sphere Method", *IGY Rocket Report Series Number 5* (1959).
14. Jones, L. M., Peterson, J. W., Schaefer, E. J., and Schulte, H. F.,
"Upper-Air Density and Temperature: Some Variations and an Abrupt Warming in the Mesosphere", *Journal of Geophysical Research*, 64, 2331-2340, (1959).
15. Kellogg, W. W. "Warming of the Polar Mesosphere and Lower Ionosphere in Winter", *RAND Report P-2032-NSF* (1960).

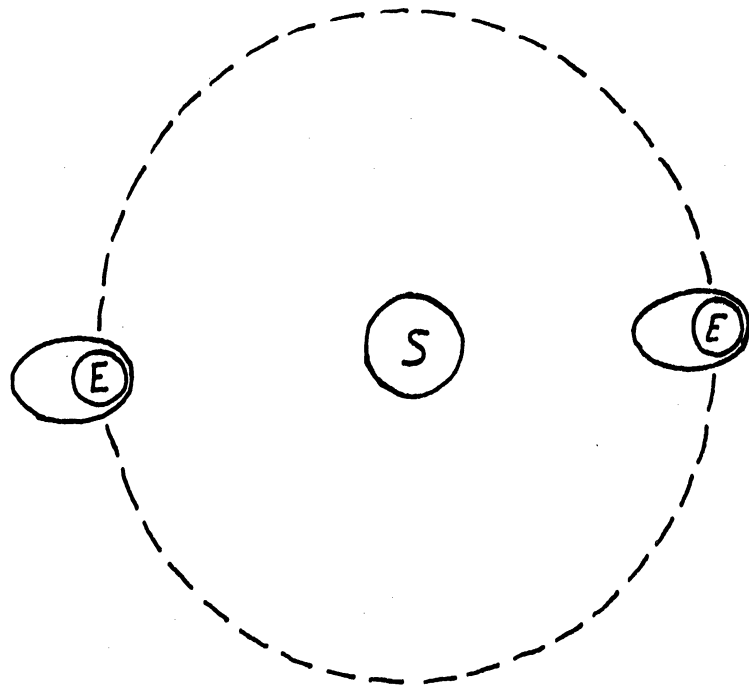


Figure 1. Annual motion of satellite perigee.

P-T-ρ AND WINDS BY GRENADES

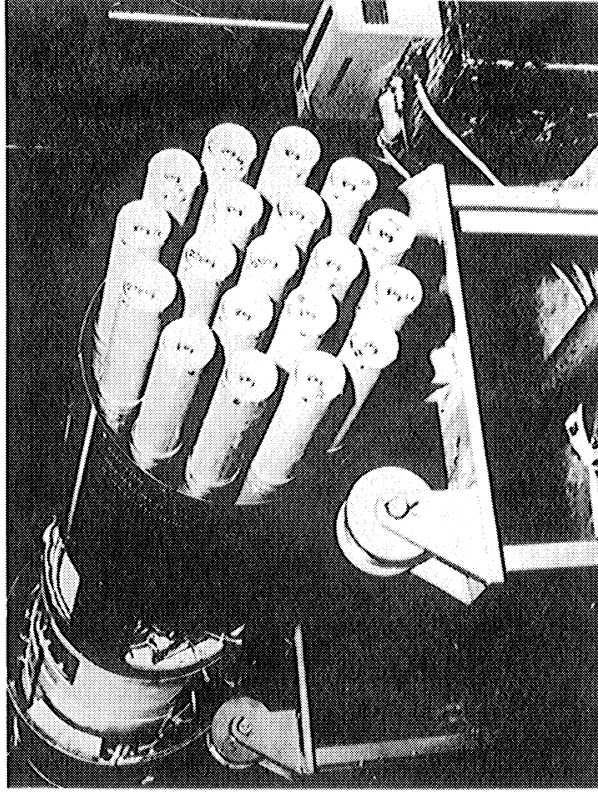
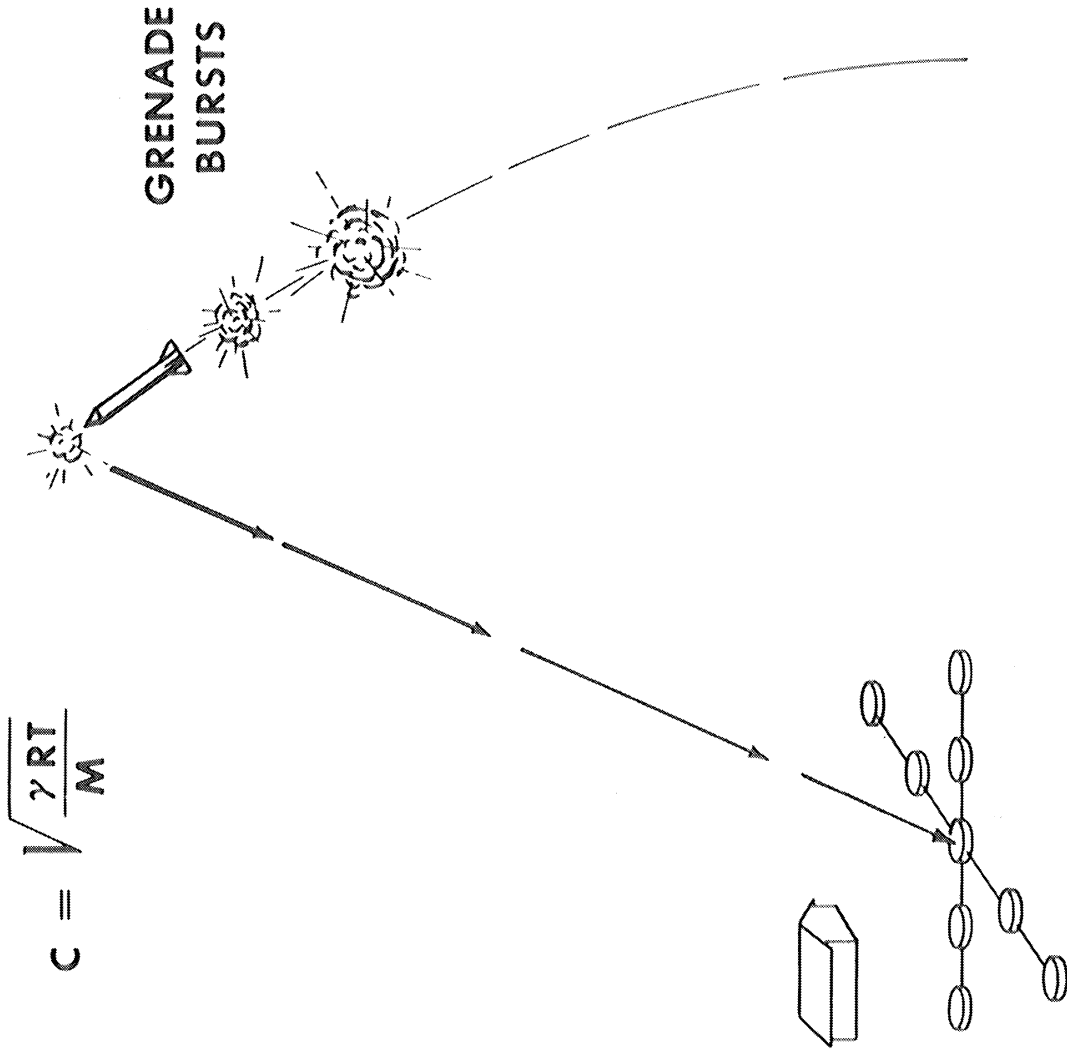


Figure 2. Rocket-grenade system. Nineteen grenades in nose of Aerobee rocket.

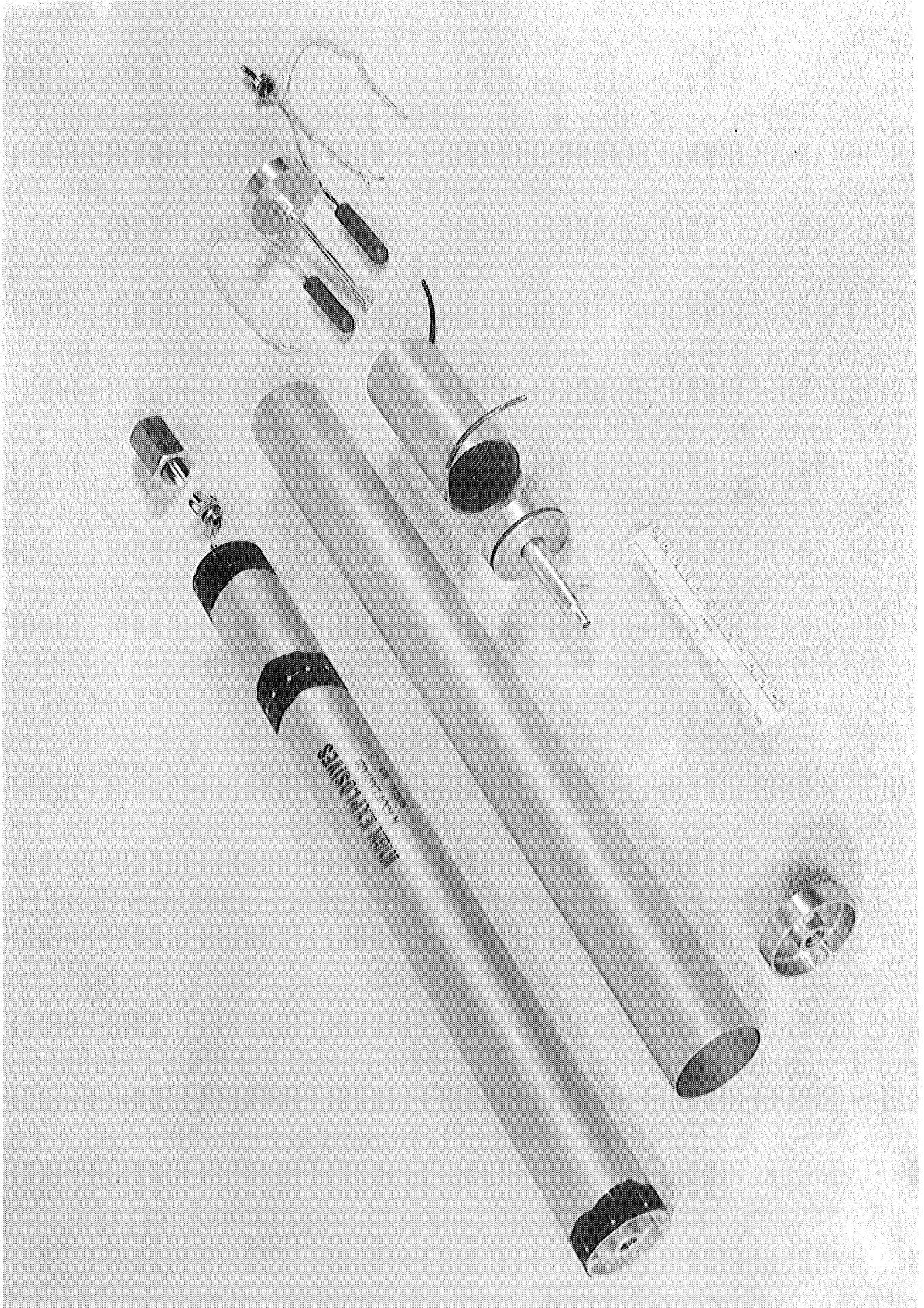


Figure 3. Component parts of grenades used in Aerobees.

ROCKET GRENADE TEMPERATURE DATA SUMMER AVERAGES
AT FT. CHURCHILL 58° 46' NORTH

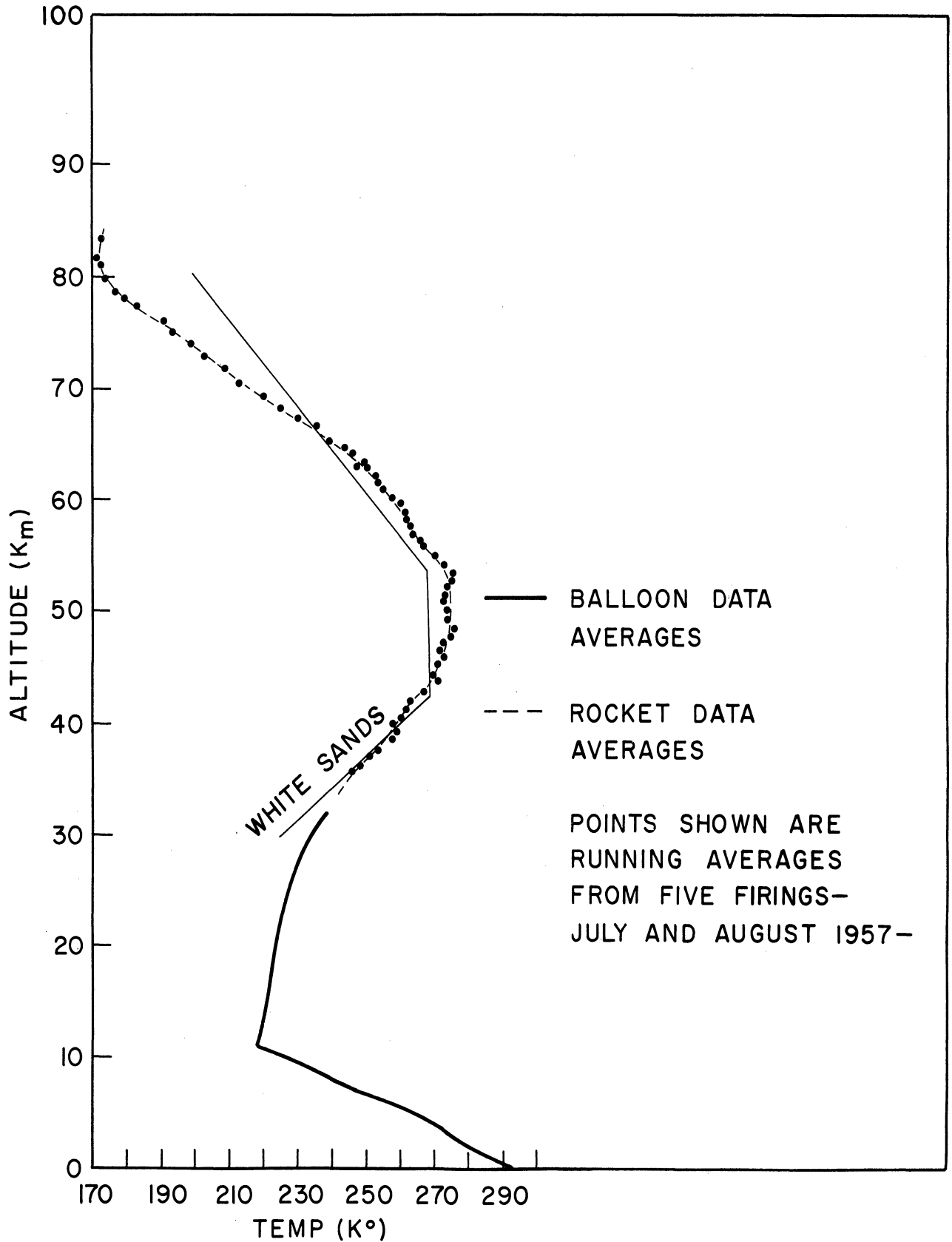


Figure 4. Summer averages of temperature data from rocket-grenade experiment at Fort Churchill, Canada. Points shown are averages from five firings.

ROCKET GRENADE TEMPERATURE DATA WINTER AVERAGES
AT FT. CHURCHILL 58° 46' NORTH

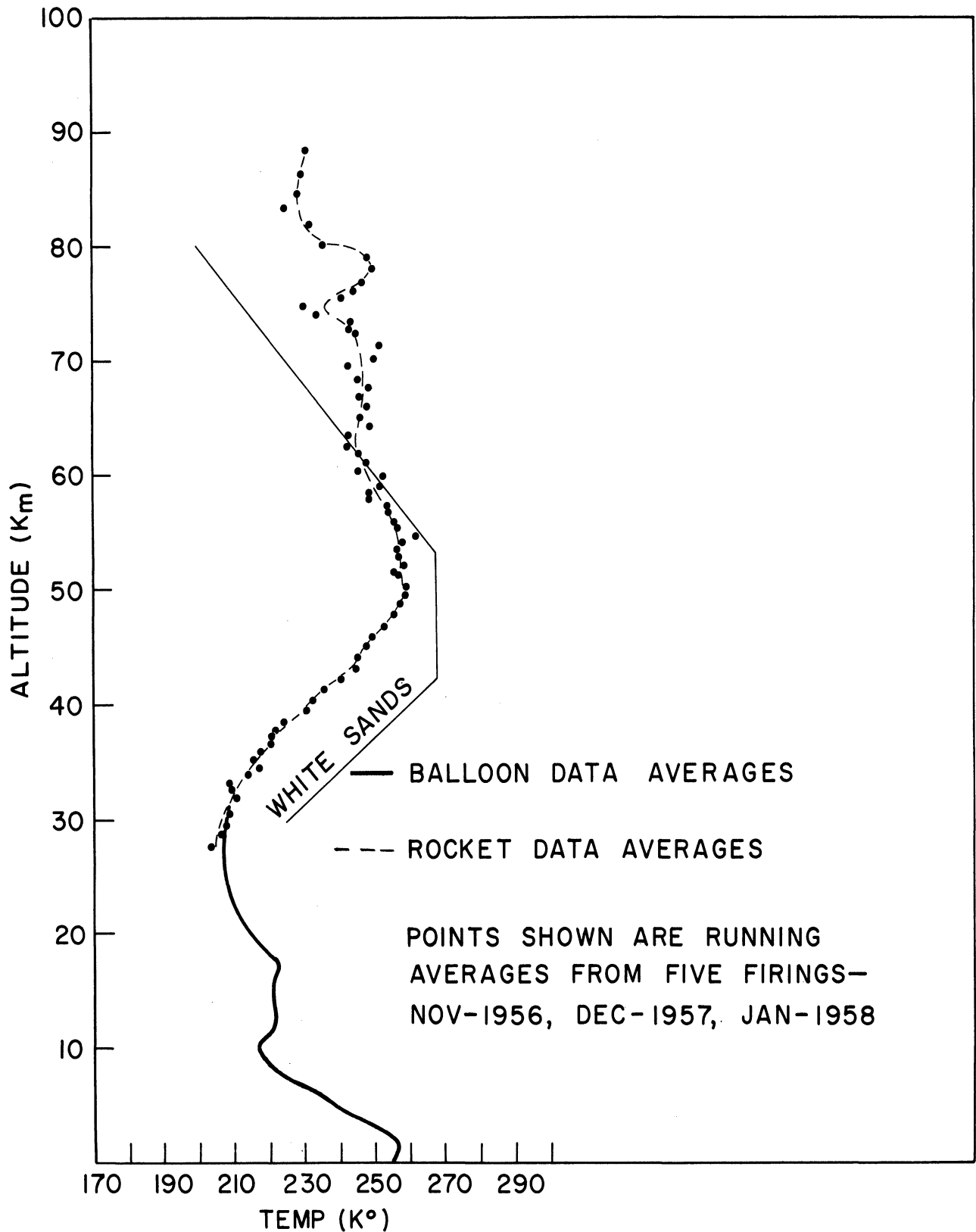


Figure 5. Winter averages of temperature data from rocket-grenade experiment at Fort Churchill, Canada. Points shown are averages from five firings.

P-T- ρ BY DRAG ON A SPHERE

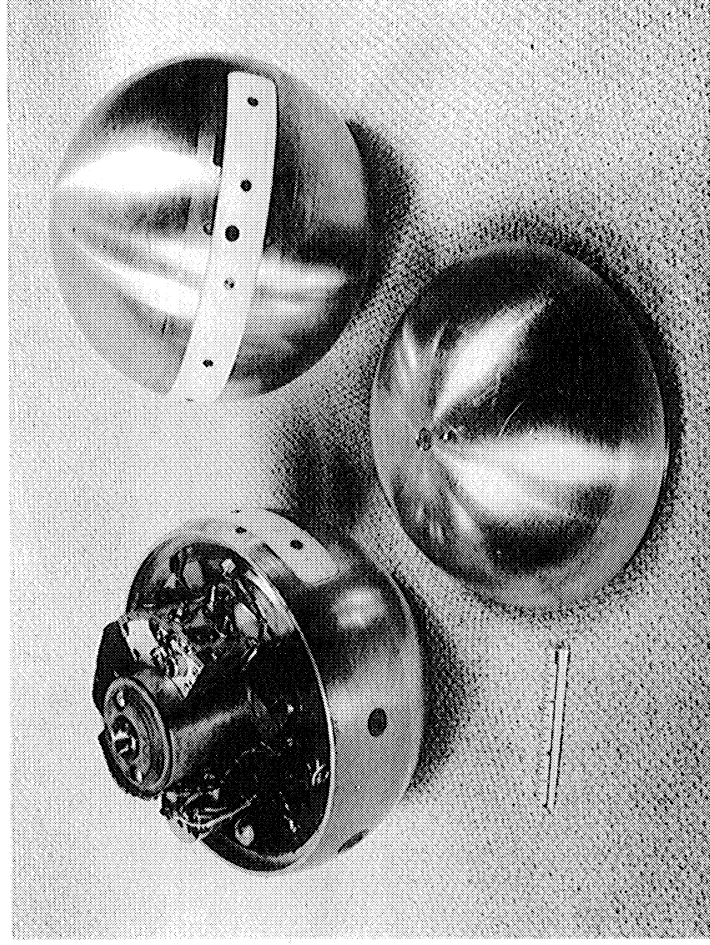
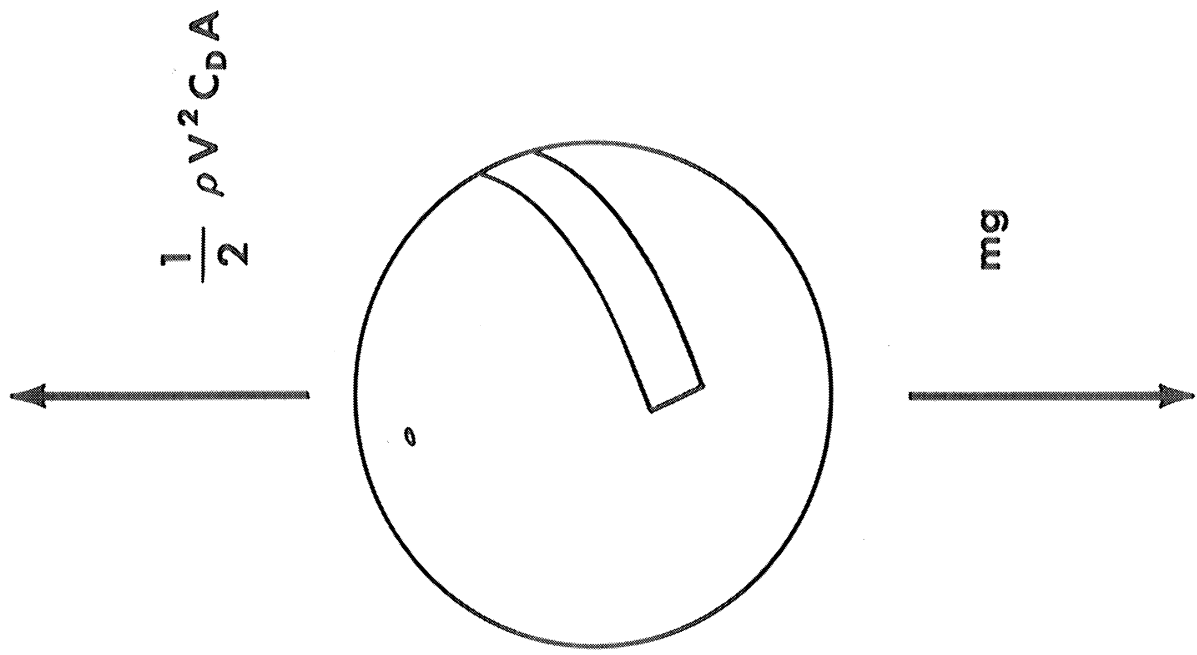


Figure 6. Seven inch eleven pound sphere containing accelerometer and telemetry equipment.

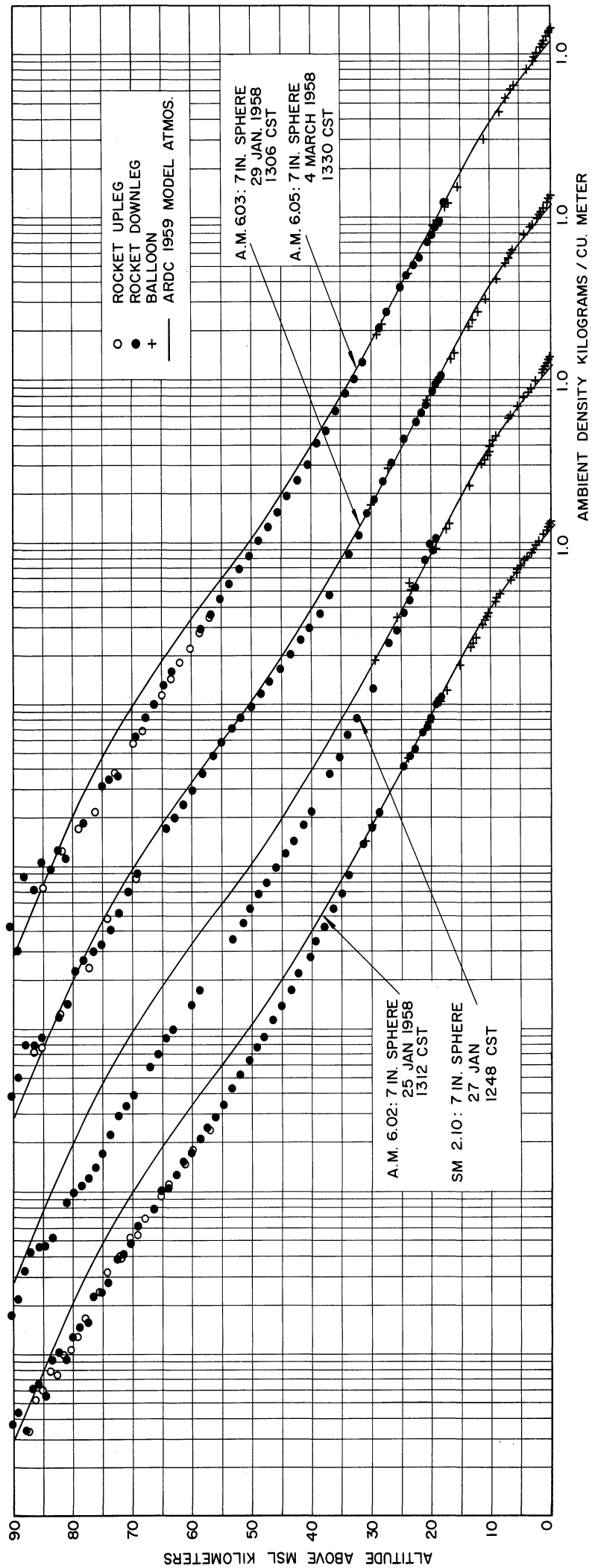


Figure 7. Upper air density. Four wintertime sphere flights at Fort Churchill, Canada. (58.7°N).

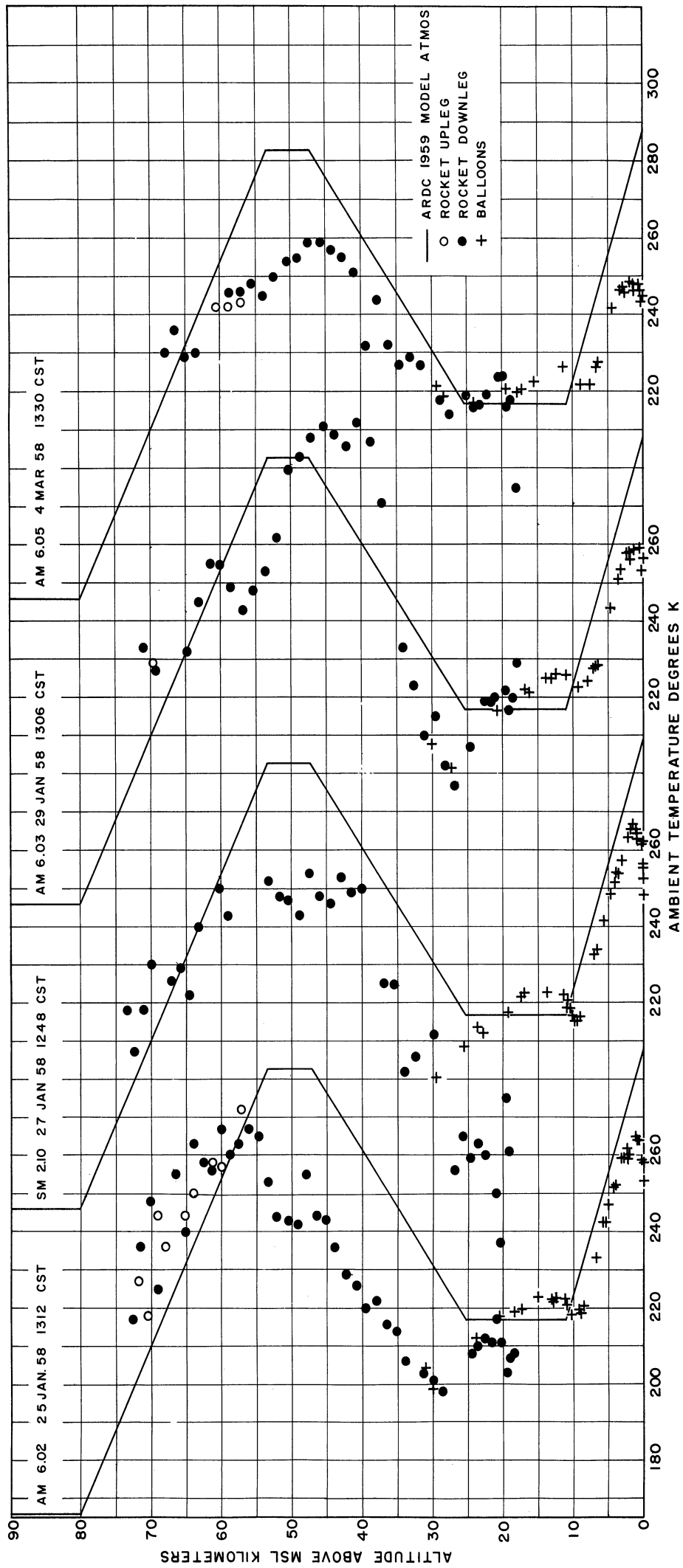


Figure 8. Upper air temperature. Four wintertime sphere flights at Fort Churchill, Canada (58.7°N).

**TEMPERATURE MEASUREMENTS AT FORT CHURCHILL, CANADA (59°N)
ON 27 AND 29 JANUARY 1958 BY ROCKET-GRENADE
AND FALLING-SPHERE EXPERIMENTS**

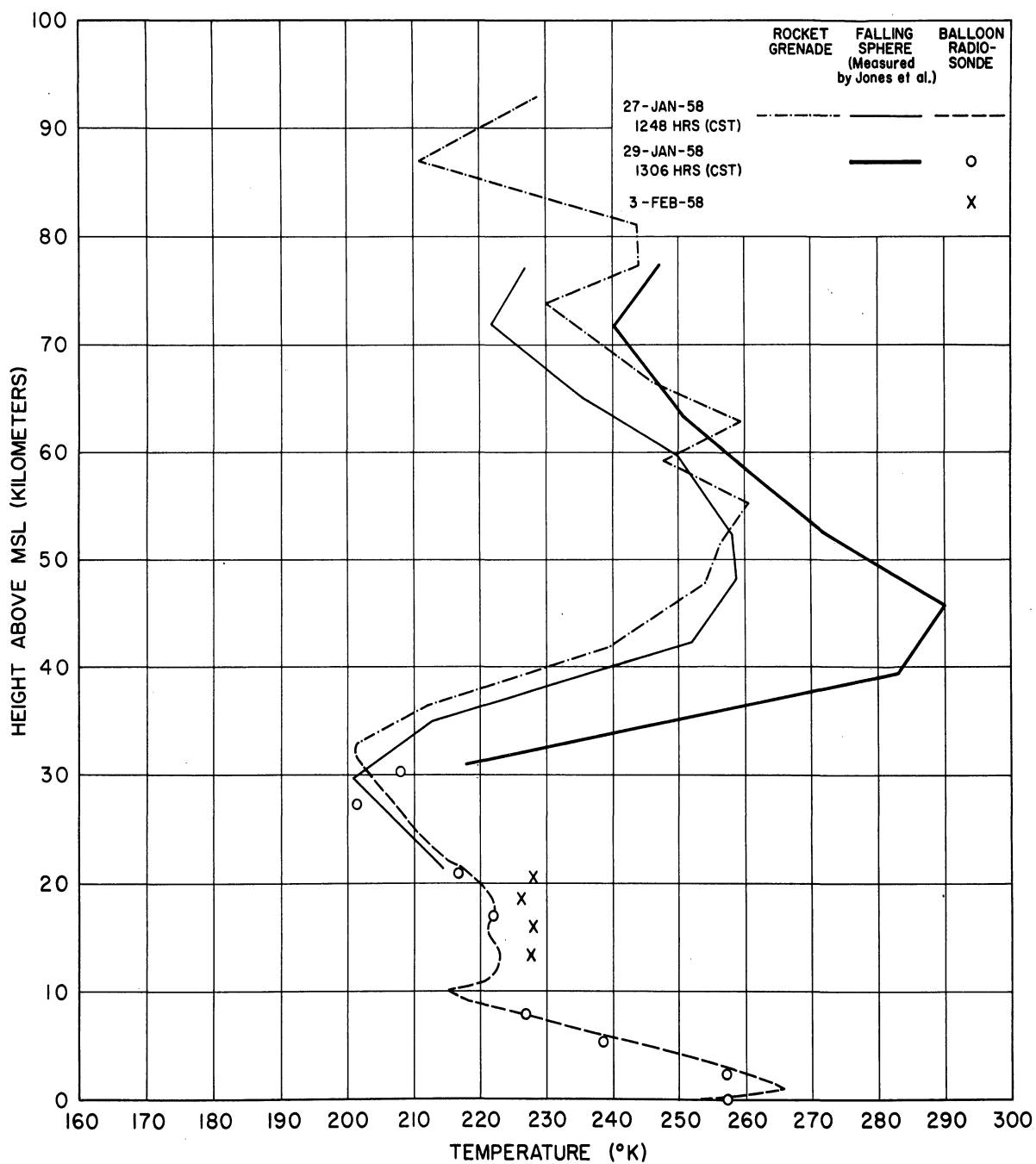


Figure 9. Temperature measurements at Fort Churchill, Canada (58.7°N) on 27 and 29 January 1958 by rocket-grenade and falling-sphere experiments.

